Journal of Fusion Energy (2022)41:5
https://doi.org/10.1007/s10894-022-00318-8

ORIGINAL RESEARCH

Analysis of Two Fusion Reactor Designs Based on Magnetic Electrostatic Plasma Confinement

B. J. Sporer[1]

Accepted: 4 April 2022

Abstract

Two fusion reactor designs based on electrostatic plugging of a magnetic cusp system—known as electromagnetic or magnetic electrostatic plasma confinement (MEPC)—are analyzed for feasibility. Both designs use the linear set of ring cusps geometry. The first design, proposed by Dolan (Current trends in international fusion research, Springer, 1997), utilizes low-temperature superconductor technology and is comparable in size to the ITER or DEMO tokamaks, while producing 500–1000 MW_{th} of fusion power. The second design is more compact, assuming more powerful magnetic fields are now conceivable with high-temperature superconductor technology, and produces 50–150 MW_{th} of fusion power. Using scaling equations from Dolan, both reactors have an estimated energy gain $Q \approx 10$ when neglecting impurities and alpha heating. A different model of conduction and diffusion losses, including the effect of minor impurities, is developed. This model predicts Q values about 3–5 times smaller than Dolan. Reactor engineering considerations such as the first wall, blanket, and magnetic forces in a linear set of ring cusps geometry are discussed. An experimental program to resolve outstanding questions and verify scaling laws is needed to determine the feasibility of an MEPC fusion reactor.

Keywords Electrostatic confinement · Electromagnetic confinement · Electrostatic plugging · MEPC · Cusp · HTS coil · High-temperature superconductor · Linear set of ring cusps

Introduction

Superior magnetohydrodynamic stability can be obtained in a magnetic confinement system with open field lines, though loss of plasma along these open field lines must be greatly inhibited somehow for a realistic net-gain reactor. As demonstrated in the tandem mirror concept [1], direct control of ambipolar electric fields can be used to reduce end losses in a magnetic mirror system.

The same control can be applied to magnetic cusp arrangements (see Figs. 1, 2), which have further stability advantages: global favorable curvature (discouraging interchange/ballooning modes) and a magnetic null region to randomize magnetic moments (discouraging loss-cone and other kinetic instabilities). With sufficient heating power, magnetic cusp-confined plasmas can remain quiescent at $\beta \rightarrow 1$ and beyond; i.e. the plasma pressure pushes out on the magnetic field and 'inflates' the cusp, forming a bulk, field-free plasma volume surrounded by a thin, magnetized sheath [2–4]. Experiments in a quasi-spherical cusp confinement device known as the "Poly-well" [5] (see Fig. 2) have shown enhanced electron confinement in the high-β 'inflated' state [6]. A disadvantage of global favorable curvature is that it requires at least one ring/line cusp, through which leakage can be excessive.

Simple tandem mirrors use separately heated plasma in two end-cells to create a potential barrier for particles leaking from the main mirror region. Alternatively, voltage can be applied directly via electrodes in contact with the leaking plasma, as shown in Fig. 3. Typically, the anode electrodes, magnet coils, and vacuum chamber are at ground potential, while cathode electrodes are positioned to reflect electrons emanating from point and ring cusps.This technique is known in the literature as electromagnetic or magnetic electrostatic plasma confinement (MEPC). MEPC has received the most attention in the Soviet Union by Oleg Lavrent'ev at the Kurchatov Institute [9], and in

✉ B. J. Sporer
bsporer@umich.edu

[1] Nuclear Engineering and Radiological Sciences, University of Michigan, Ann Arbor, MI 48109, USA

Published online: 18 April 2022

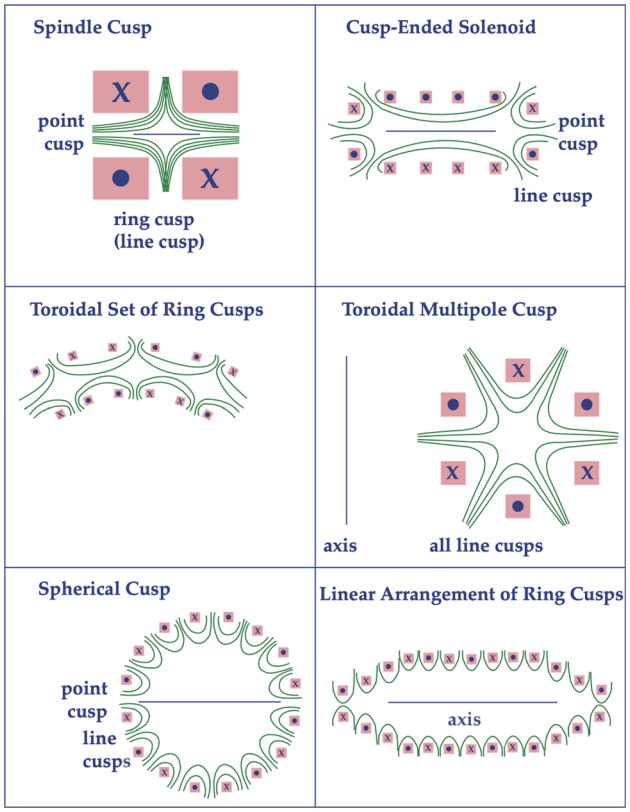

Fig. 1 Various magnetic cusp arrangements for plasma confinement. Figure reproduced from Dolan [7]

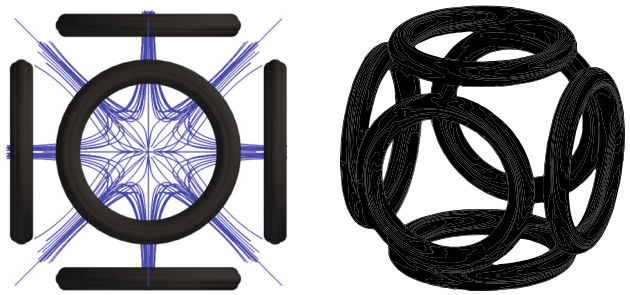

Fig. 2 The "Polywell" is another quasi-spherical cusp confinement arrangement. An embodiment of MEPC, the concept utilizes electron space charge to confine ions and has shown enhanced electron confinement at high-β. Figure reproduced from Park [8]

the United States by Thomas Dolan. In the 1990s, Dolan wrote an excellent summary and scaling analysis of MEPC [7, 10], inspiring this work.

Lavrent'ev, whose fusion proposals inspired Andrei Sakharov, continued to advocate for an MEPC/electromagnetic thermonuclear reactor that he called "Elemag" [11] until his death in 2011. The Elemag reactor point design is very consistent with Dolan's scaling analysis.

This work will consider the thermonuclear and engineering implications of the MEPC reactor envisaged by Dolan [10], as well as a more compact reactor design

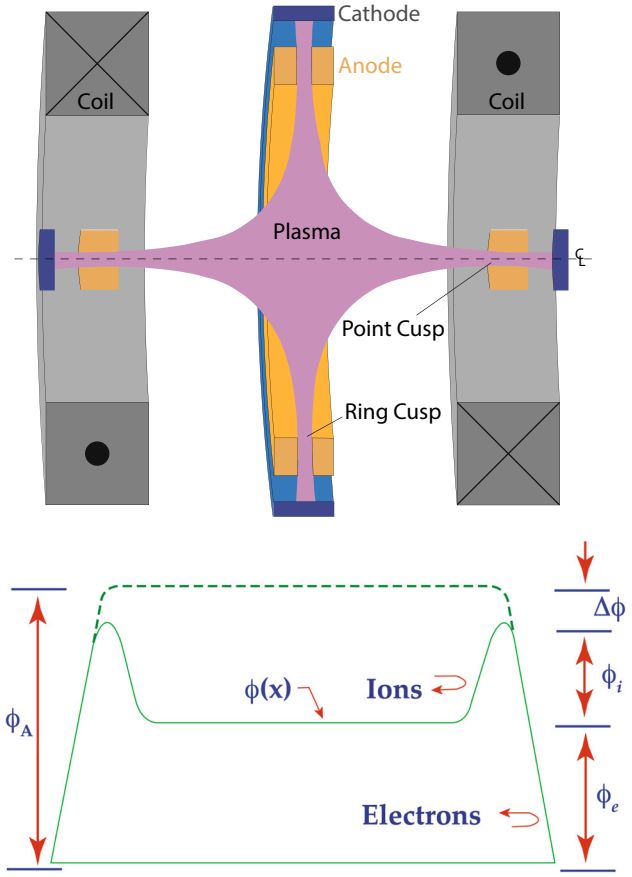

Fig. 3 Basic geometry and electric potential distribution of magnetic electrostatic plasma confinement in a spindle cusp. The dashed line is the vacuum potential with no plasma present. $\Delta\phi$ is the self-shielding potential due to space charge effects, ϕ_i is the potential barrier for ions, and ϕ_e is the potential barrier for electrons. The sum of these three potentials is equal to the applied voltage, ϕ_A. Figure reproduced from Dolan [7]

which may be possible considering recent advances with high-temperature superconductor (HTS) technology.

Electric Pressure Requirements in MEPC Cusps

Before discussing the reactor designs, a common concern with electromagnetic confinement should be rebutted. Fusion reactor concepts proposing any sort of electrostatic confinement of the plasma can be suspicious, since the plasma pressure at usable fusion power density would far exceed conceivable electric pressure. For example, the electric field required to match the pressure of a plasma with $n_e = n_i = 10^{20}$ m^{-3} and T = 10 keV would be 2.7 MV/cm, which is unrealistic to sustain in a reactor environment for a net-gain burn duration.

However, with careful consideration of the Maxwell stress tensor, it has been shown theoretically and

computationally [12] that the magnitude of the electric field required for pressure balance is reduced when the plasma has dimensions smaller than the local Debye length. Such can often be the case in MEPC, where the electric field merely assists magnetic confinement, and where the reduced-density, anisotropic plasma streaming through the cusps may have a half-width comparable to the electron gyroradius.

The reduced electric pressure required for confinement in MEPC is:

$$p_E = \frac{\epsilon_0}{2} E_{\max}^2 = \frac{1}{4}\left(\frac{\delta}{\lambda_D}\right)^2 \cdot p_p, \quad (1)$$

where δ is the half-width of the plasma streaming through the cusps, λ_D is the local Debye length in the plasma stream, and $p_p = n_e k T_e + n_i k T_i$ is the local plasma pressure. With thermonuclear MEPC parameters, the required electric pressure may be reduced by a factor 4–20, bringing the corresponding applied voltages into the realm of feasibility.

Perhaps the greatest uncertainty in pursuing an MEPC reactor lies with the sustainable voltages and electric fields (and behavior of electrical insulators) in the high-radiation environment. Similar risks are encountered in supersonic rotating mirror and stabilized field-reversed fusion concepts [13, 14].

Though the plasma streaming through the cusps (mostly relativistic electrons) in MEPC is ostensibly non-Maxwellian and anisotropic, the dominant cusp-region instabilities encountered in MEPC experiments thus far are diocotron (Kelvin–Helmholtz) oscillations due to $\mathbf{E} \times \mathbf{B}$ shear. These, and other two-stream-type instabilities one might expect, may actually play a beneficial role by selectively removing lower-energy, trapped electrons from the cusp regions. These trapped electrons do not contribute to bulk plasma density, but they do contribute to space charge in the gap and the self-shielding voltage drop $\Delta\phi$ (see Fig. 3). Since the trapped electrons cannot energetically reach the bulk plasma, their active removal does not affect bulk plasma velocity-space.

While electric pressure balance is not imposed explicitly, the following reactor design analysis does account for the effect of electron space charge streaming through the cusps. This space charge effect sets the primary limitation on electron plasma density in MEPC.

Selection of HTS Reactor Parameters

For engineering simplicity, and to maximize the volume of field-free plasma per leaky cusp, a linear set of ring cusps is the preferred MEPC reactor geometry, as in Fig. 4. Circa

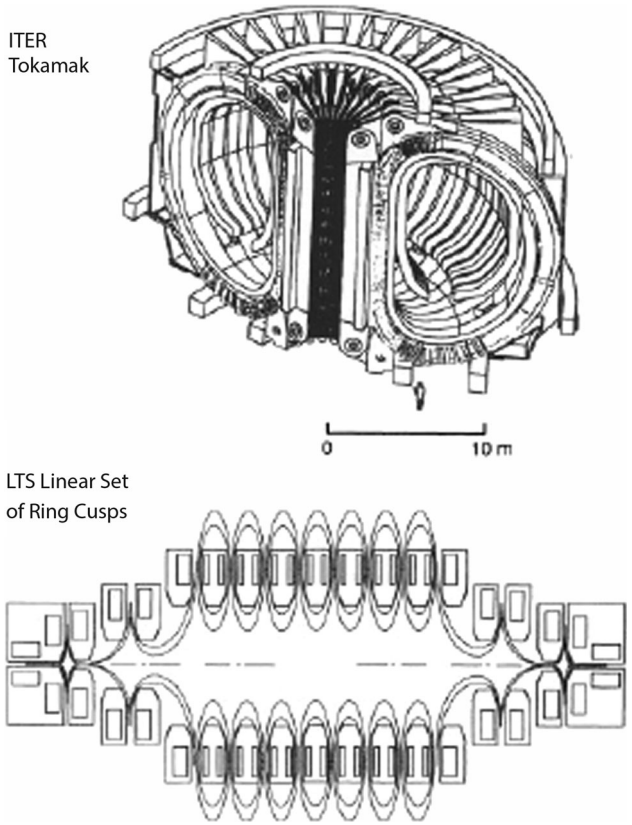

Fig. 4 A net-gain MEPC reactor (bottom) using a linear set of twelve ring cusps—at the scale envisioned by Dolan—in comparison with the ITER tokamak (top). Reflecting electrode structures for the MEPC reactor are not shown, but would be located in the cusp regions. Figure reproduced from Dolan [10]

1997, Dolan presented a reactor concept using low-temperature superconducting (LTS) magnets to produce a field of 6 tesla in the cusps (see Table 1).

However, recent advancements with high-temperature superconductor (HTS) technology may allow a more compact, high-field MEPC reactor—analogous to the ARC/SPARC tokamak designs [15]. Furthermore, due to the simple axisymmetric geometry of a linear set of ring cusps, even higher on-plasma fields than expected in the SPARC tokamak ($\sim$12 tesla [16]) might be achievable.

A single, SPARC-scale HTS toroidal field coil was recently tested by Commonwealth Fusion Systems (CFS) in collaboration with the Plasma Science & Fusion Center at MIT, and demonstrated an on-coil magnetic field of 20 tesla [17] in nominal operation. The University of Wisconsin (in parternership with CFS/MIT) has received an ARPA-E grant to build an HTS magnetic mirror (WHAM) capable of 17 tesla across 5 cm bores, with a breakeven reactor design calling for 25 tesla across 30 cm bores [18]. In fact, HTS solenoids with fields > 40 tesla have been designed [19], and 100 tesla HTS magnets shown to be technically feasible [20].

Table 1 Two sets of MEPC reactor parameters

Parameter	Dolan LTS design [10]	New HTS design
B-field in ring cusps B_a [T]	6	16
Applied voltage ϕ_a [kV]	400	500
Anode gap spacing d [mm]	4	4
Plasma electron density n_e [m^{-3}]	1.1×10^{20}	2.9×10^{20}
Plasma temperature $T_e \sim T_i$ [keV]	20	25
Coil/cusp radius R [m]	3.5	0.83
Plasma length L [m]	36	10
Dolan scaling relation gain Q	10	10

A cusp field strength of $B_a = 16$ tesla will be used as the basis for a second MEPC reactor design. Perhaps even higher fields are imaginable with HTS in the near future, but ultimately the limiting factor in HTS coil design is mechanical stress. Tolerable material stress, not HTS current density, limits the maximum field of a high-field reactor concept like SPARC [21]. Tolerable stress in the MEPC geometry is difficult to constrain without comprehensive coil engineering analysis.

The factor which limits MEPC plasma density is not the beta ratio as in tokamaks, but space charge limits in the anode/cusp gaps, where the applied electric fields must not be too distorted. Analyzing a variety of effects including acceleration and diocotron oscillations, Dolan estimates the electron density in the gaps will be approximately an order of magnitude lower than the bulk plasma density. He also conservatively assumes a Lorentzian-shaped electron density profile in the gap with half-width $w = 2\rho_e$, where ρ_e is the electron gyroradius in the anode/cusp field. Assuming these relations hold, the maximum bulk plasma electron density n_e while keeping the self-shielding voltage drop $\Delta\phi \leq 100$ kV is approximately:

$$n_e \leq 3.5 \times 10^{20} \frac{B_a}{d_{\mathrm{mm}} \sqrt{T_{e,\mathrm{keV}}}}, \tag{2}$$

where $T_{e,\mathrm{keV}}$ is the central plasma electron temperature in keV and d_{mm} is the anode gap in millimeters. For cusp field $B_a = 16$ tesla, plasma temperature $T_e = 25$ keV, and anode gap $d = 4$ mm, the maximum plasma electron density is $n_e = 2.9 \times 10^{20}$ m^{-3}. This electron density will be used for the high-field reactor design (see Table 1).

As mentioned in the previous section, a significant area of concern in MEPC is maintenance of the applied voltage in proximity of dense, hot plasma and radiation. The larger the applied voltage ϕ_a, the greater the plasma temperature and the reactor gain Q. Dolan estimates the bulk plasma temperature as $T_e \approx T_i \approx 0.05\, e\phi_a$, using $\phi_a = 400$ kV for a plasma temperature of 20 keV in his LTS design.

There is precedent for maintenance of up to 500 kV applied voltage in the PSP-2 rotating mirror plasma experiment [14]. Lavrent'ev uses 600 kV in the latest Elemag design [11], and theoretically higher magnetic field strength with HTS might allow maintenance of higher voltages. With further consideration of advances in high-voltage and pulsed-power technology since 1997, use of 500 kV and 25 keV plasma temperature for the HTS design is motivated.

Finally, Dolan provides a simple scaling relation from Yushmanov [22] for the energy gain factor Q of an MEPC linear set of ring cusps reactor. This relation does not take into account alpha trapping & heating, which would increase the gain factor. Nor does it take into account energy losses due to neutral gas collisions or impurities, which would decrease the gain factor. Assuming a reasonable fraction of trapped electrons in the anode gaps, Dolan/Yushmanov's gain relation can be written simply as:

$$Q \approx 3 \times 10^{-6}\, B_a\, \phi_a^2\, R, \tag{3}$$

with ϕ_a in kV, which gives $Q \approx 10$ for the LTS design with cusp/coil radius $R = 3.5$ m. R is selected to be 0.83 m for the HTS design to give $Q \approx 10$ as well. Note, using the other HTS parameters, a fairly small machine with radius only 0.17 m is required for $Q \approx 2$, the minimum expected gain of the SPARC tokamak [15].

The parameters for Dolan's LTS reactor design ($B_a = 6$ T, $\phi_a = 400$ kV) and the new HTS design ($B_a = 16$ T, $\phi_a = 500$ kV) determined in this section are summarized in Table 1.

Plasma Volume and Surface Area in a Linear Set of Ring Cusps

To further evaluate the reactor designs, the plasma volume and surface area of the designs will be needed. These can be calculated by assuming a given plasma profile in a linear set of ring cusps. The plasma in one-half of one cusp region might have a profile as shown in Fig. 5. An exponential profile $r(z) = z^{\gamma} + r_p$ is assumed, where r_p is the radius of the bulk plasma.

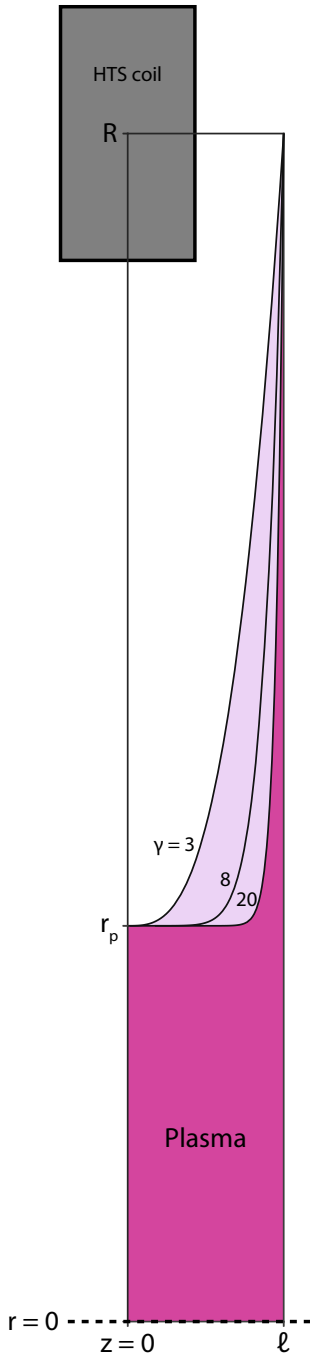

Fig. 5 Hypothetical plasma surface profile of one cusp half-region within a linear set of ring cusps. An exponential-shaped profile $r(z) = z^{\gamma} + r_p$ is assumed to calculate the plasma volume and surface area. This figure, with $R = 3r_p$ and $l = 0.2(R - r_p)$, may be approximately to scale for an HTS prototype reactor

Assuming a first-generation reactor design might have $R \sim 3r_p$ as shown in Fig. 5, the volume V_s of the plasma section is:

$$V_s = \Gamma_v \cdot \pi R^2 l, \tag{4}$$

where

$$\Gamma_v = \frac{4}{9(2\gamma + 1)} + \frac{4}{9(\gamma + 1)} + \frac{1}{9} \tag{5}$$

The surface area S_s of the plasma section is:

$$S_s = \Gamma_s \cdot 2\pi R l, \tag{6}$$

where

$$\Gamma_s = \frac{2}{3(\gamma + 1)} + \frac{1}{3}. \tag{7}$$

Since the total plasma length $L = N_c \cdot l$ (from Table 1) with number of ring cusps $N_c \gg 1$, the total plasma volume and surface area is approximately:

$$V = \Gamma_v \cdot \pi R^2 L \tag{8}$$

$$S = \Gamma_s \cdot 2\pi R L. \tag{9}$$

Note the plasma volume for the LTS design is 280 m^3, one-third that of the ITER tokamak [23]. Γ_v and Γ_s are weak functions of γ, taking values of Γ_v = 0.28–0.14 and Γ_s = 0.50–0.37 for γ = 3–20. For the remainder of this paper, $\Gamma_v = 0.2$ and $\Gamma_s = 0.4$ will be used.

Fusion Power and Radiation Losses

The DT fusion power of each design is:

$$P_{\text{fus}} = n_D\, n_T\, \langle \sigma v \rangle_{DT} \times\ 17.6\ \text{MeV} \times \Gamma_v \cdot \pi R^2 L. \tag{10}$$

The achievable DT fuel density in an MEPC reactor will be sensitive to the impurity level, because electrons have the density limit for effective electric confinement. So at this point, an assumption must be made on impurities in MEPC plasmas.

Unfortunately, high-Z ions will be well-confined electrostatically. Though some methods of impurity and ash removal have been proposed [7], impurity build-up remains a primary concern for an MEPC reactor. If no effective means of removal can be found, periodic shutdown and restart of the reactor may be required.

For 5% helium + 1% beryllium impurity ($Z_{\text{eff}} = 1.20$), the number densities are $n_D = n_T = 4.5 \times 10^{19}$ m^{-3} for the LTS reactor and 1.2×10^{20} m^{-3} for the HTS reactor. The total DT fusion powers are then 670 MW and 100 MW for LTS and HTS, respectively. Since the Dolan/Yushmanov energy gain Q and aspect ratio $\frac{L}{R}$ are approximately the same for both designs, one sees how the stronger fields enabled by HTS suggest medium-power, more compact reactors—a demand recognized already in the fission reactor industry.

Note that the real fusion power will be slightly less than the quoted values since the ion Maxwellian distribution is diminished for energies greater than $e\phi_i$ (see

"Section Conduction and Diffusion Losses"), reducing the normal reactivity parameter $\langle \sigma v \rangle$ for a given temperature. This weak effect has been quantified by Dolan [24], and should not affect the conclusions of this work.

An analysis of alpha particle trajectories in a high-β cusp reactor has not been performed to the author's knowledge. Partial alpha confinement would enhance the gain factor Q from the value listed in Table 1. Assuming the first wall can be made more than one alpha particle gyroradius from the edge of the plasma, some significant alpha confinement and heating may occur. Though, many alphas directed along open field lines will impact the anode region before shedding much energy to the plasma. With total alpha confinement, the alpha heating powers are 130 MW and 20 MW for LTS and HTS, respectively. Interestingly, even with total alpha loss to the first wall, $\sim 5\%$ of alpha energy will be recovered directly as electricity to the power source that is ultimately maintaining the negative potential of the bulk plasma.

Cyclotron radiation losses are assumed to be negligible since most of the plasma in cusp confinement is unmagnetized. Bremsstrahlung radiation loss is given by:

$$P_{\text{brems}} = A_{\text{brems}}\, n_e^2\, Z_{\text{eff}}\, \sqrt{kT_e} \times \Gamma_v \cdot \pi R^2 L, \tag{11}$$

where $A_{\text{brems}} = 1.6 \times 10^{-38}\ \frac{\text{Wm}^3}{\sqrt{\text{eV}}}$. For $Z_{\text{eff}} = 1.20$, the bremsstrahlung power is 8.7 MW for the LTS reactor and 1.1 MW for the HTS reactor. With the approximation $n_D = n_T \approx \frac{n_e}{2Z_{\text{eff}}}$, the bremsstrahlung power as a fraction of fusion power is shown for each design in Fig. 6. The HTS design is slightly more robust to bremsstrahlung losses at large Z_{eff} due to the higher operating temperature.

Because an MEPC reactor would operate at high temperature, bremsstrahlung radiation is not such a concern with impurities as is reduction of the DT fuel density (and therefore fusion power density). The fusion power would scale roughly as $\frac{1}{Z_{\text{eff}}^2}$ for a constant electron density.

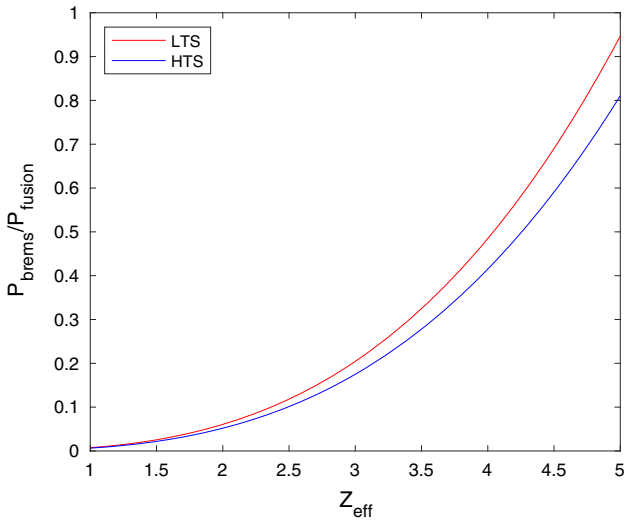

Fig. 6 Ratio of bremsstrahlung to fusion power as a function of Z_{eff} for each reactor design, with the approximation $n_D = n_T \approx \frac{n_e}{2Z_{\text{eff}}}$

Conduction and Diffusion Losses

Plasma energy is primarily lost through conduction and diffusion. Electrons and ions upscattered over their respective potential barriers will quickly leak through a cusp and be lost to the cathodes. Additionally, electrons trapped in the magnetized edge layer will diffuse across the magnetic field until they impact the anode region or first wall.

Cohen et al. [25] derives an expression for open-field line particle loss rates over potential barriers based on the analytic treatments of Pastukhov, Chernin, and Rosenbluth. In his analysis [7], Dolan uses these loss rates to define a characteristic conduction time, which he combines with the edge-trapping and diffusion times for an overall energy confinement time.

A different model of conduction and diffusion losses will be explored here for comparison. However, this model is not entirely self-consistent because it uses the plasma temperature and potential barrier heights estimated semi-empirically by Dolan et al. [7]. Electron losses will be considered first, with the ion loss rate set to match the electron loss rate for charge conservation.

Since $e\phi_a \gg T_e$, the electron energy distribution is approximately Maxwellian, but diminished at energies greater than $e\phi_e$. Each electron energy collision time, τ_E^{ee}, one-tenth of the electrons which would fill the truncated region of the Maxwellian are assumed to be lost over the electron potential barrier ϕ_e to the cathode. The one-tenth factor arises from the assumption that bulk plasma electron density is an order of magnitude greater than the electron density penetrating the cusp/anode gaps.

Therefore, the electron conduction energy loss rate is:

$$P_{\text{cond},e} = 0.1 \cdot \frac{E_e^* - N_e^* e\phi_e}{\tau_E^{ee}}, \tag{12}$$

where

$$E_e^* = \frac{2N_e kT_e}{\sqrt{\pi}} \cdot \Gamma\left(\frac{5}{2}, \frac{e\phi_e}{kT_e}\right) \tag{13}$$

is the electron thermal energy in the diminished region of the Maxwellian at temperature T_e with total plasma electron inventory $N_e = n_e \times \Gamma_v \pi R^2 L$. Not to be confused with the plasma profile factors Γ_v and Γ_s, $\Gamma(a,x)$ is the incomplete gamma function—a result of the Maxwellian integration. $\phi_e = \phi_a - \Delta\phi - \phi_i$ is the potential barrier for

electrons (see Fig. 3). It is assumed $\phi_e \approx 0.5\phi_a$ as in Dolan [7]. Additionally:

$$N_e^* = \frac{2N_e}{\sqrt{\pi}} \cdot \Gamma\left(\frac{3}{2}, \frac{e\phi_e}{kT_e}\right) \tag{14}$$

is the number of electrons in the diminished region. The factor $N_e^* e\phi_e$ in the energy loss rate equation accounts for the fact that conduction losses are to the cathode, which is at a potential difference ϕ_e from the bulk plasma (shifting the particle energies just before loss).

The electron energy collision time from Stacey [26] with $\ln\Lambda = 17.5$ can be written as:

$$\tau_E^{ee} = 6.1 \times 10^{14} \ \frac{T_{e,\mathrm{keV}}^{\frac{3}{2}}}{n_e}. \tag{15}$$

Assuming $T_e = 0.05\, e\phi_a$ as in Dolan, the electron conduction energy loss rate is estimated to be 3.3 MW and 340 kW for the LTS and HTS designs, respectively. The power is relatively low because electrons have little kinetic energy left upon cathode impact, having surmounted their potential barrier.

Ion confinement in MEPC is almost completely electrostatic, but electrons are lost by diffusion across the magnetic field. Assuming that a fraction $(1 - e^{-1}) = 0.63$ of the thermal electron energy is lost each diffusion time τ_{diff}, the electron diffusion energy loss rate is:

$$P_{\mathrm{diff}} = 0.95 \cdot \frac{N_e kT_e}{\tau_{\mathrm{diff}}}. \tag{16}$$

The great achievement of MEPC and cusps is near-classical confinement, ostensibly due to the global stability advantages mentioned in "Section Introduction". The Jupiter-2M linear set of seven ring cusps achieved diffusion time of approximately half the classical prediction [27]. Introducing this factor of one-half to the classical confinement time as estimated by Pastukhov [28] and assuming $T_e \sim T_i$ in the central plasma gives:

$$\tau_{\mathrm{diff}} \sim 0.11 \cdot \frac{\tau_{ei} V d}{S \rho_{e,a}\, \rho_{e,p}}, \tag{17}$$

where $\tau_{ei} = 4.3 \times 10^{14} \ \frac{T_{e,\mathrm{keV}}^{\frac{3}{2}}}{n_i Z_{\mathrm{eff}}^2}$ is the electron-ion momentum collision time from Stacey [26] with $\ln\Lambda = 17.5$, V is the plasma volume, S is the plasma surface area, $\rho_{e,a} = \frac{\sqrt{2m_e kT_e}}{eB_a}$ is the electron gyroradius in the anode gap, and $\rho_{e,p} = \sqrt{\frac{m_e}{2\mu_0 e^2 n_e}}$ is the electron gyroradius at the bulk plasma boundary (where local $\beta = 1$).

The ratio $\frac{V}{SR}$ of the plasma is:

$$\frac{V}{SR} = \frac{\Gamma_v}{2\,\Gamma_s}, \tag{18}$$

which is an even weaker function of γ than Γ_v or Γ_s individually, taking values of $\frac{V}{SR}$= 0.3–0.2 for γ= 3–20.

Using a value of $\frac{V}{SR}$= 0.25 reduces the diffusion time equation to:

$$\tau_{\mathrm{diff}} \sim 2.7 \times 10^{-2} \ \frac{\tau_{ei} R d}{\rho_{e,a}\, \rho_{e,p}}. \tag{19}$$

Thus, for the LTS design, $\tau_{\mathrm{diff}} = 3.8$ s. For the HTS design, $\tau_{\mathrm{diff}} = 1.8$ s. Using these values, the electron diffusion energy loss rates are 24 MW and 2.6 MW for the LTS and HTS designs, respectively.

Ion conduction losses are estimated based on charge conservation. Ions lost to the cathode will have an average energy:

$$\overline{E}_{\mathrm{cond},i} = \frac{E_i^*}{N_i^*} + e\phi_e, \tag{20}$$

where E_i^* and N_i^* take the form of the electron diminished Maxwellian region equations (Eqs. 13–14), but use the ion potential barrier $\phi_i \approx 0.3\,\phi_a$ (as in Dolan [7]) when evaluating the incomplete gamma functions. The factor $e\phi_e$ accounts for the fact that ion losses are to the cathode, and ions are accelerated before impact.

Assuming total alpha confinement, ion charge will be lost via conduction at the same rate electron charge is lost via conduction and diffusion:

$$\dot{N}_{\mathrm{cond},i} = \frac{1}{Z_{\mathrm{eff}}} \left[0.1 \ \frac{N_e^*}{\tau_E^{ee}} + 0.63 \ \frac{N_e}{\tau_{\mathrm{diff}}}\right], \tag{21}$$

assuming a fraction $(1 - e^{-1}) = 0.63$ of plasma electrons are lost each diffusion time. The ion conduction energy loss rate is:

$$P_{\mathrm{cond},i} = \overline{E}_{\mathrm{cond},i} \cdot \dot{N}_{\mathrm{cond},i}, \tag{22}$$

which gives 270 MW and 30 MW for the LTS and HTS designs, respectively.

The energetics of the two reactor designs as calculated in the last two sections ("Sections Fusion Power and Radiation Losses and Conduction and Diffusion Losses") are organized in Table 2. The gains with no alpha confinement are a factor of 3–5 lower than predicted by Dolan/Yushmanov's relation. This is likely in part due to use of a smaller characteristic electron-ion collision time and consideration of impurities. Also, the electron conduction and diffusion losses are added linearly in this model, unlike in Dolan where the characteristic timescales are added reciprocally. Since the two electron loss processes act on the same population and are not independent of each other, the reciprocal method may be more appropriate.

In both designs, loss of electron charge is dominated by diffusion. Loss of energy is dominated by ion conduction, due to acceleration into the cathode. In an advanced design,

Table 2 Energetics of the two MEPC reactor designs with the new conduction and diffusion models and $Z_{\text{eff}} = 1.20$

Parameter	Dolan LTS design [10]	New HTS design
Fusion Power [MW]	670	100
Max Alpha Heating [MW]	130	20
Bremsstrahlung Power Loss [MW]	8.7	1.1
Diffusion Power Loss [MW]	24	2.6
Conduction Power Loss (e^-) [MW]	3.3	0.34
Conduction Power Loss (i^+) [MW]	270	30
Gain (no α confinement)	2.2	3.0
Gain (total α confinement)	3.8	7.1

perhaps the cathode could be made semi-transparent to lost ions, such that they impact a different surface near ground potential. In theory, this might recover a large fraction of the ion energy and increase the energy gain of the system by a substantial factor.

Plasma Startup, Auxiliary Heating, and Fueling

Another advantage of MEPC is that the plasma can be heated relatively simply and efficiently by electron beam injection from the cathodes. In the Jupiter-2M experiment, over 80% of electron beam energy appeared in the plasma [7]. Beam current could be controlled by modulation of cathode gun voltage or temperature in point or ring cusps. Ion losses tend to be minimal at the point cusps due to angular momentum from $\mathbf{E} \times \mathbf{B}$ rotation of the plasma [29].

Since the majority of plasma is not magnetized, RF heating does not seem ideal, but may have limited use. Strong electron resonance heating in the anode gaps could possibly reduce the cold, trapped electron population, and therefore reduce the self-shielding voltage drop $\Delta\phi$, leading to better confinement scaling. Cyclotron heating in the gaps could also reduce general electron leakage by "spinning up" electrons as they approach the cusp hole (driving them out of the loss-cone by increasing $v_\perp$). Applied RF could also influence diocotron oscillations. The electron cyclotron fundamental frequency in the anode gaps would be around 170 GHz for 6 tesla LTS and 450 GHz for 16 tesla HTS, ignoring relativistic effects.

As with many magnetic confinement concepts, neutral beam heating could be a suitable option for heating and refueling an MEPC reactor. However, hot ion confinement would be similar to alpha confinement in that collisions must slow the ions to below the ion potential barrier ϕ_i in only a few radial transits, or else leakage out of a cusp is likely. Also, it could be difficult to engineer neutral beam input ports in the geometry of a linear set of ring cusps.

Initial particle inventory could be provided by burnout of neutral gas fill by electron beam, though gas puffs for refueling are not recommended since neutral collisions would increase the diffusion rate of electrons in the sheath. As with tokamaks, pellet injection could be a good refueling option.

With no alpha confinement, the required auxiliary heating power is 310 MW and 34 MW for the LTS and HTS designs, respectively. This could correspond to electron beam currents of 770 A and 67 A from the cathodes of each design. The electron injection currents would constitute a tiny fraction of the electron space charge passing through the anode gaps. Other methods of heating, as well as partial alpha confinement, could contribute to the input power requirement.

Dolan/Yushmanov's model predicts $Q \approx 10$ for both designs. Interestingly, with the new conduction & diffusion model presented here, the HTS design shows a larger gain than that of the LTS design. This could suggest it is easier to reach ignition in MEPC with a high-field, compact design.

First Wall, Blanket, and Tritium Breeding

The first wall surface area can be conservatively estimated as the plasma surface area:

$$A_w = \Gamma_s \cdot 2\pi RL. \tag{23}$$

Therefore, the areal neutron power to the first wall would be approximately 1.7 MW/m^2 for the LTS design and 3.8 MW/m^2 for the HTS design. The 'enhanced', beryllium-armored copper/steel tiles in mind for the ITER first wall are capable of 4.7 MW/m^2 neutron power [30], and a similar technology could be used in an MEPC reactor. Unlike in tokamaks, there should be no edge-localized modes (ELMs) or disruption-like events in the cusp

geometry that would deposit excessive or unpredictable amounts of energy directly to the first wall.

Liquid lithium, lead-lithium, or some molten salt formulation could flow through tubes in the wall as a primary coolant and blanket, extracting the neutron heat and breeding tritium at a minimum rate of 4.3 and 0.64 grams per hour to match the consumption of the LTS and HTS designs, respectively. Each breeding event with lithium-6 produces an additional 4.8 MeV, enhancing the neutron heating power in the blanket by 35%. Uranium or other actinides could be dissolved in the primary coolant (e.g., FLiBe with dissolved uranium tetrafluoride as in some molten salt reactor designs [31]) to further boost heat output in a fission-fusion hybrid or actinide-burner scheme.

Behind the blanket, a lower-temperature coolant and vacuum radiation shield region could separate the cryostat containing the magnet coils. Considering the high current density and on-coil fields desired with HTS, liquid helium would likely be needed for both designs. If the coils were made larger with reduced engineering current density, liquid hydrogen might be an option for HTS. There could also be increased temperature margin for quenching with the HTS design.

Active cooling would also be needed for the cathodes, which see a small amount of neutron power but a great deal of conduction heating—primarily via impact of high-energy ions. The cathodes could be cooled with the primary coolant as well, or a separate coolant loop, depending on the desired operating temperature. Cathode surface area may be somewhat arbitrary, since the diverging field beyond the cusp acts as a natural divertor (similar to magnetic mirrors). If the arc length of each cathode surface is 20 cm for both designs with twelve ring cusps, the total cathode surface area is:

$$A_c = 24\pi \cdot (R + \delta R) \cdot 20 \text{ cm}, \tag{24}$$

where $\delta R \sim 20$ cm represents the larger radius of the cathodes as compared with the coil radius, R. Therefore, the areal conduction power to the cathodes is 5.0 MW/m^2 for the LTS design and 1.9 MW/m^2 for the HTS design. Sputtering is not as concerning at the cathode since any liberated ions would be immediately pulled back, so the cathode could possibly be a high-Z material like tungsten. Erosion and ion implantation will be a concern, and the cathodes would probably need frequent replacement.

The anode surfaces will see most of the diffusion loss thermal power. Assuming the height of the anode surface $h = 10\,d$ (the maximum recommended by Yushmanov), the total anode surface area is approximately:

$$A_a \approx 480\pi \cdot d \cdot R. \tag{25}$$

Therefore, the areal diffusion power to the anodes is is 1.1 MW/m^2 for the LTS design and 0.53 MW/m^2 for the HTS design. Anode sputtering could be a primary impurity source in MEPC; luckily, few plasma ions can energetically reach the anodes.

High-voltage grading between the anode and cathode should be used to reduce the chance of insulator flashover. The insulator would likely be made of a ceramic appropriate for the reactor environment such as alumina or a carbide.

A sketch of a possible hardware design suggesting ~ 16 tesla cusp fields (assuming 1000 A/mm^2 engineering current density is possible with the HTS coils as in SPARC [15], but ignoring magnet structural considerations) is shown in Fig. 7.

For an MEPC reactor, pushing to higher field strengths with HTS technology has another engineering advantage. While the magnetic pressure scales as B_a^2, the bulk plasma pressure can only scale as B_a due to space charge restrictions in the anode gaps. Thus, by increasing B_a, the bulk plasma surface is moved physically farther from the coils, while the cusp/anode gaps can remain a set distance. This essentially elongates the cusps when depicted to scale (see Fig. 7), stretching them outward radially so as to allow a greater volume of first wall, blanket, coolant, and shielding between the coils and the plasma. The cusp/anode gaps can

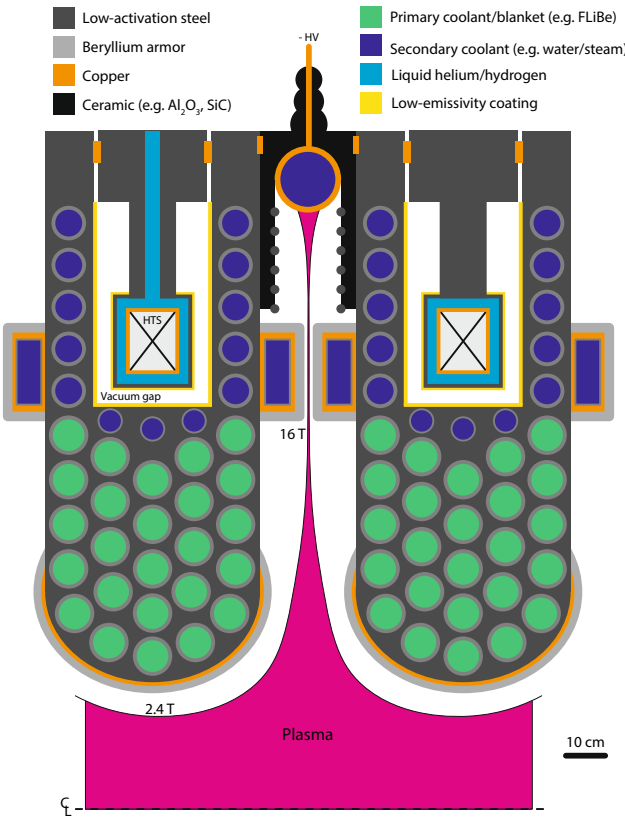

Fig. 7 Engineering design sketch of one ring cusp region for a high-field MEPC reactor utilizing HTS coils

remain close to the coils (<35 cm for HTS), taking advantage of the high fields there, because few hot ions exist in this region to produce damaging neutrons.

Stored Plasma and Magnetic Energies

Ignoring the effects of impurities, the energy stored in the plasma of each design is:

$$E_p = \frac{3}{2}\, n_e\, k\, (T_e + T_i) \cdot \Gamma_v \cdot \pi R^2 L, \tag{26}$$

which gives 260 MJ for the LTS design and 14 MJ for the HTS design. For comparison, the energy stored in the ITER plasma will be approximately 350 MJ.

The magnetic energy of a linear set of twelve ring cusps can be very roughly approximated as the energy of thirteen toroids carrying uniform current, with major radius R and minor radius $a = \sqrt{\frac{I_{\text{coil}}}{\pi J_e}}$. The engineering current density J_e is estimated as 100 $\frac{\text{A}}{\text{mm}^2}$ for LTS [32] and 1000 $\frac{\text{A}}{\text{mm}^2}$ for HTS. The total current in the coil cross-section is estimated as $I_{\text{coil}} = \frac{\pi L B_a}{24\,\mu_0}$ to produce $\frac{B_a}{2}$ per coil in the cusps. Thus, the total magnetic energy is:

$$E_B = 13 \cdot \frac{1}{2} L_{\text{coil}} I_{\text{coil}}^2, \tag{27}$$

with each coil loop inductance given by:

$$L_{\text{coil}} \approx \mu_0 R \left(\ln \frac{8R}{a} - 2 \right), \tag{28}$$

which gives 38 GJ and 4.7 GJ for the LTS and HTS designs, respectively. The stored magnetic energy of the ITER tokamak will be around 50 GJ. The HTS coils would be at minimum 15 cm thick, producing 8 tesla *each* in the cusp about 35 cm from the surface of the coil (see Fig. 7 for rough scale).

In a linear set of ring cusps (under normal operation), only the two coils on the ends of the reactor will see a large net force axially. The axial repulsive force on an end HTS coil in a thirteen coil system can be expressed as the summation of forces from the other twelve coils:

$$F = \frac{12 \mu_0 I_{\text{coil}}^2 R}{L} \cdot \sum_{n=1}^{12} \frac{(-1)^{n+1}}{n} \approx 230\ \text{MN} \tag{29}$$

Verifying the above estimate, a magnetostatic simulation in Computer Simulation Technology (CST) Studio Suite predicts a force of 200 MN between two toroidal coils with the HTS design parameters and maximum HTS engineering current density (1000 $\frac{\text{A}}{\text{mm}^2}$). A force of 200 MN may seem enormous, but the total centripetal force reacted by the ITER cylindrical vault from the 18 toroidal coils exceeds 400 MN [33]. Assuming a 400 MPa yield strength, $\sim$0.5 m^2 of steel would be needed to restrain the HTS coils—e.g., seven solid bars with 30 cm diameter.

The ITER centripetal forces are partly managed with six fiberglass pre-compression rings, each 5 m in diameter, because metal would not be magnetically or cryogenically compatible [34]. For the linear set of ring cusps design, coil support probably does not need to be cryogenically compatible. An external clamping frame made of many steel bars could hold the coil structure together. In the result of an uncontrollable coil quench, other coils could see strong net forces which must be managed by the external frame as well. Advanced quench detection and control on a reactor-scale HTS coil system would mitigate this risk. In conclusion, magnetic coil stresses in an HTS linear set of ring cusps would be an engineering challenge, but would not be too dissimilar to those in other large magnetic confinement reactor concepts.

MEPC Reactor Concerns

There are several unresolved questions in MEPC which must be investigated before a reactor could be confidently designed. Primary concerns are listed below. Each of these issues has already been identified by Dolan [10].

- *Plasma Purity.* Perhaps the greatest issue facing an MEPC reactor is build-up of high-Z impurities, which would be well-confined electrostatically. Maintenance of clean plasma at fusion temperatures in MEPC must be assessed and methods of impurity and ash removal developed; otherwise, periodic shutdown and restart of the reactor may be required. Since MEPC reactors would operate at high temperature, bremsstrahlung radiation is not the primary concern with impurities. The major concern is reduction of DT fuel density, due to constraints on electron density in MEPC.
- *Voltage Holding.* Maintenance of large applied voltages (100–600 kV) must be demonstrated in the MEPC geometry, while in the presence of hot plasma and radiation. Sputtering control, voltage grading, and electrically insulating materials compatible with reactor engineering will need more investigation.
- *Electron Transport.* Encouragingly, diffusion at only twice the classical rate was observed in the Jupiter-2M experiment, but some other MEPC experiments (e.g., the toroidal ATOLL experiment) have shown anomalous transport—presumably due to ion acoustic and hybrid drift modes [7]. Good symmetry and a large volume of field-free plasma in the linear set of ring cusps geometry seems to be advantageous for micro-

stability. Nonetheless, transport rates at reactor-relevant density and magnetic fields must be investigated.

- *Alpha Confinement.* If the first wall is located more than one alpha gyroradius (12 cm for the HTS design) away from the plasma surface, alpha particles should be partially confined. More assessment of alpha trajectories in the linear set of ring cusps geometry is needed. Partial alpha confinement would enhance the gain beyond the Q values of Table 1.
- *Structure & Alignment.* Vacuum pump-out and the (quenching) magnet coils would apply large, transient forces to the reactor structure. These force changes must be managed simultaneously with precise alignment of electrodes and insulation of high-voltage. This represents a significant engineering and materials challenge, even in the relatively simple geometry of a linear set of ring cusps.

Conclusions and Suggestions for Future Work

Two MEPC fusion reactor designs using low-temperature and high-temperature superconducting technology have been investigated based on the summary works of Dolan and others. An alternate model of conduction and diffusion losses, including minor impurities, shows reduced gain, but reaches similar conclusions as Dolan. The LTS reactor design from Dolan is of similar magnitude to the ITER or DEMO tokamaks. In analogy to the ARC/SPARC tokamaks, HTS technology is shown to enable a more compact, medium-power reactor design with MEPC as well.

Engineering and material concerns of an MEPC reactor would be similar to other magnetic confinement concepts (e.g., tokamaks, mirrors), but could be simplified in some ways. A possible blanket and shielding concept is shown in Fig. 7. More research is needed on insulation materials and high-voltage holding in the reactor environment, a concern not just in MEPC, but also in other fusion-directed concepts such as rotating mirrors.

As with many alternative concepts, MEPC experiments have suffered low budgets and limited attention. This has constrained experiment size to <1 meter, pulsed magnetic fields to <2 tesla, and applied voltages to <10 kV. A quasi-static, high-field, high-voltage experimental campaign is needed to confirm scaling theories and address unresolved questions in MEPC.

One such low-budget experiment could be a pulsed linear set of ring cusps with $B_a \sim 4$ tesla, applied $\phi_a \sim 100$ kV, and coil pulse time of at least one second. Key experimental studies to improve scaling predictions could investigate the fraction of electron density penetrating the cusps, the potential well depth and temperature at different applied voltages, diocotron (Kelvin–Helmholtz) oscillations in the anode gaps, and high-voltage maintenance in the radiation environment.

Another valuable MEPC experiment could be a spindle cusp (a single ring cusp) made of two superconducting coils and with large applied voltage. With a cusp field $B_a > 6$ tesla and an applied voltage $\phi_a \sim 100$ kV at sufficient power, the central plasma parameters could exceed 5 keV and 10^{20} m^{-3}, producing copious neutrons even with deuterium fuel. Insight gained on such a device could be sufficient to more confidently extrapolate to reactor parameters. Such a spindle cusp could be constructed using two HTS pancake coil assemblies, such as those supplied by Commonwealth Fusion Systems for the Wisconsin HTS Axisymmetric Mirror (WHAM). These coil assemblies are capable of producing 17 tesla across their 5 cm warm bores.

With imminent advancements in HTS coil technology, and if the scaling properties of Dolan and others can be verified at high-field, high-voltage parameters, then a fusion power reactor based on MEPC may be feasible.

Acknowledgements The author would like to thank Dr. Thomas Dolan for inspiring this work with previous review articles on MEPC, and for providing feedback on the draft. The author would also like to thank Dr. Ryan McBride for proofreading the draft and providing valuable feedback.

Funding The author did not receive support from any organization for the submitted work.

Availability of data and materials Data sharing not applicable to this article as no datasets were generated or analysed during the current study

Declarations

Conflict of interest The author declares no conflict of interest.

References

1. T.C. Simonen, Summary of results from the Tandem Mirror Experiment (TMX). Technical report, Lawrence Livermore National Lab., CA (USA) (1981)
2. H. Grad, Plasma trapping in cusped geometries. Phys. Rev. Lett. **4**(5), 222 (1960)
3. J.L. Tuck, A new plasma confinement geometry. Nature **187**(4740), 863–864 (1960)
4. T.J. McGuire, Compact fusion reactor, CFR. Phys. Plasmas **22**, 070901 (2015)
5. N.A. Krall, M. Coleman, K. Maffei, J. Lovberg, R. Jacobsen, R.W. Bussard, Forming and maintaining a potential well in a quasispherical magnetic trap. Phys. Plasmas **2**(1), 146–158 (1995)
6. J. Park, N.A. Krall, P.E. Sieck, D.T. Offermann, M. Skillicorn, A. Sanchez, K. Davis, E. Alderson, G. Lapenta, High-energy

electron confinement in a magnetic cusp configuration. Phys. Rev. X **5**(2), 10 (2015)
7. T.J. Dolan, Magnetic electrostatic plasma confinement. Plasma Phys. Control. Fus. **36**(10), 1539 (1994)
8. J. Park, Polywell—a path to electrostatic fusion. EMC2, 16th US-Japan Workshop on Fusion Neutron Sources for Nuclear Assay and Alternate Applications (2014)
9. A.D. Komarov, O.A. Lavrentiev, V.A. Naboka, V.A. Potapenko, I.A. Stepanenko, Electrostatic Plasma Confinement in the Yupiter-1A Electromagnetic Trap. Ukrainskij Fizicheskij Zhurnal **25**(5), 776–780 (1980)
10. T.J. Dolan. Prospects of magnetic electrostatic plasma confinement, in *Current Trends in International Fusion Research*, pp. 197–209. Springer (1997)
11. O.A. Lavrent'ev, V.A. Maslov, S.V. Germanova, M.G. Nozdrachov, V.P. Oboznyj, B.A. Shevchuk, Modeling of a starting mode of thermonuclear reactor "Elemag." Fusion Sci Technol **47**(1T), 224–227 (2005)
12. A.A. Ware, J.E. Faulkner, Electrostatic plugging of open-ended magnetic containment systems. Nucl. Fusion **9**(4), 353 (1969)
13. C. Romero-Talamás, I. Abel, J. Ball, D. Basu, B. Beaudoin, L. Dorsey, N. Eschbach, A. Hassam, T. Koeth, Z. Short, et al., Overview of the Centrifugal Mirror Fusion Experiment (CMFX). *Bulletin of the American Physical Society* (2021)
14. G.F. Abdrashitov, A.V. Beloborodov, V.I. Volosov, V.V. Kubarev, Y.S. Popov, Y.N. Yudin, Hot rotating plasma in the PSP-2 experiment. Nucl. Fusion **31**(7), 1275 (1991)
15. A.J. Creely, M.J. Greenwald, S.B. Ballinger, D. Brunner, J. Canik, J. Doody, T. Fülöp, D.T. Garnier, R. Granetz, T.K. Gray et al., Overview of the SPARC tokamak. J. Plasma Phys. **86**(5), 10 (2020)
16. M. Greenwald, D. Whyte, P. Bonoli, Z. Hartwig, J. Irby, B. LaBombard, E. Marmar, J. Minervini, M. Takayasu, J. Terry, et al. The high-field path to practical fusion energy. PSFC Report PSFC/RR-18-2 (2018)
17. D. Chandler, MIT-designed project achieves major advance toward Fusion Energy. https://news.mit.edu/2021/MIT-CFS-major-advance-toward-fusion-energy-0908. Accessed 08 Sept 2021
18. C. Forest, J. Anderson, B. Mumgaard, D. Whyte. The Wisconsin HTS Axisymmetric Mirror (WHAM). ARPA-E BETHE Kickoff Virtual Workshop (2020)
19. H. Bai, M.D. Bird, L.D. Cooley, I.R. Dixon, K.L. Kim, D.C. Larbalestier, W.S. Marshall, U.P. Trociewitz, H.W. Weijers, D.V. Abraimov et al., The 40 T superconducting magnet project at the National high magnetic field laboratory. IEEE Trans. Appl. Supercond. **30**(4), 1–5 (2020)
20. Y. Iwasa, S. Hahn, First-cut design of an all-superconducting 100-T direct current magnet. Appl. Phys. Lett. **103**(25), 253507 (2013)
21. Q&A session with Brandon Sorbom of Commonwealth Fusion Systems, APS Division of Plasma Physics Meeting 2020
22. E.E. Yushmanov, The power gain factor Q of an ideal magneto-electrostatic fusion reactor. Nucl. Fusion **20**(1), 3 (1980)
23. The ITER Organization. Facts & figures. https://www.iter.org/factsfigures (2021). Accessed 14 Nov 2021
24. T.J. Dolan, B.L. Stansfield, *Fusion reaction rate from truncated Maxwellian distributions*. Technical report, Univ. of Quebec, Varennes (1973)
25. R.H. Cohen, M.E. Rensink, T.A. Cutler, A.A. Mirin, Collisional loss of electrostatically confined species in a magnetic mirror. Nucl. Fusion **18**(9), 1229 (1978)
26. W.M. Stacey, *Fusion: An Introduction to the Physics and Technology of Magnetic Confinement Fusion* (Wiley, New York, 2010)
27. S.A. Vdovin, S.B. Germanova, O.A. Lavrent'ev, V.A. Maslov, M.G. Nozdrachev, V.P. Obozniy, V.I. Petrenko, N.N. Sappa. Plasma accumulation and confinement in the Jupiter-2M multicusp electromagnetic trap, in *Proceedings All Union Conference on Open Traps*, pp. 70–81 (1990)
28. V.P. Pastukhov, Classical transport processes in a magnetoelectrostatic trap. Fizika Plazmy **4**(3), 560–569 (1978)
29. O.A. Lavrent'ev, Diffusion loss of particles and energy in a one-slit electromagnetic trap. Ukrainskij Fizicheskij Zhurnal **26**(9), 1466–1472 (1981)
30. Fabricating ITER's first wall. https://www.neimagazine.com/features/featurefabricating-iters-first-wall-4551656/. Accessed 06 April 2021
31. J. Uhlíř, M. Mareček, M. Straka, L. Szatmáry, Z. Novỳ, P. Sláma, P. Svoboda, P. Toman, Experimental verification of selected processes devoted to MSR fuel cycle technology (2016)
32. Y. Zhai, P. Titus, C. Kessel, L. El-Guebaly, Conceptual magnet design study for fusion nuclear science facility. Fusion Eng. Des. **135**, 324–336 (2018)
33. H. Rajainmaki, A. Foussat, J. Rodriguez, D. Evans, J. Fanthome, M. Losasso, V. Diaz, The ITER pre-compression rings–a first in cryogenic composite technology, in *AIP Conference Proceedings*, vol. 1574, pp. 92–99. American Institute of Physics (2014)
34. J. Knaster, W. Baker, L. Bettinali, C. Jong, K. Mallick, C. Nardi, H. Rajainmaki, P. Rossi, L. Semeraro, Design Issues of the Pre-compression Rings of ITER, in *AIP Conference Proceedings*, vol. 1219, pp. 145–154. American Institute of Physics (2010)